

## Effects of Drying Temperature on the Optical Properties of Solution Derived (Pb,La)TiO<sub>3</sub> Thin Films

Dae Sung Yoon, Sung Wuk Kim, Jun-Mo Koo, Zhong Tao Jiang,  
Byeong-Soo Bae, Won Jong Lee, Kwangsoo No and Sang Hee Cho\*

Dept. of Mater. Sci. and Eng., Korea Advanced Institute of Sci. and Tech.,  
Kusong-dong 373-1, Yusong-gu, Taejeon 305-701, Korea

\*Dept. of Inorg. Mater. Eng., Kyungpook National Univ., Buk-gu, Taegu 702-701, Korea  
(Received December 7, 1995)

Using sol-gel processing method, thin films of lathanum modified lead titanate (PLT) on Corning 7059 glass were prepared. A differential thermal analysis (DTA/TG) curve of gel powder and infrared spectra (FT-IR) of the films were measured to estimate residual organics in them. The heat-treated films were characterized by X-ray diffraction (XRD). Microstructures of the films were observed by a scanning electron microscope (SEM). Optical properties of the films were determined by a UV-VIS spectrophotometer. The waveguiding properties and optical attenuation were measured with the end coupling method and the cut back method. Effects of the drying conditions on the transmittance and the propagation loss of the films were investigated. Experimental results showed that the content of residual organics in the film decreased as the drying temperature of the film increased. As the La content of the film increased, the grain size decreased and the transmittance increased. The transmittances of the films increased with the increasing of the drying temperature. The propagation losses in the film decreased as the drying temperature increased.

**Key words :** PLT thin film, Sol-gel, Waveguide, Propagation loss

### I. Introduction

Recent years have brought renewed interest in integrated-optical applications of ferroelectric thin films.<sup>1-9)</sup> The ferroelectric films have several potential advantages for electro-optic or nonlinear optical applications over the standard technology using diffused or ion exchanged waveguides in single-crystal materials such as lithium niobate and lithium tantalate. These potential advantages include compatibility with a variety of substrates, low processing temperatures, easy manufacture at low cost and capability of deposition over large area. On the other hand, fabricating the films of good enough optical quality to permit waveguiding over long distances has proved to be difficult.

There have been many recent advances in the technology of deposition of thin films of lathanum modified lead titanate (PLT) and related ferroelectric films.<sup>1-11)</sup> The ferroelectric PLT films exhibit both excellent transparency and strong electro-optic effects. A few researchers have tried to fabricate the PLT thin films for the waveguide application using the sputtering method.<sup>1-4)</sup> The propagation losses of the sputter-deposited PLT film, however, are too high (approximately 5~15 dB/cm), which is possibly due to the larger grain size by using the high deposition temperature. The degree of homogeneity of sputter-deposited films is lower than that of solution derived films. Recently, Teowee<sup>6,7)</sup> reported that

the small grain size of the crystalline film inherent in the low temperature sol-gel processing contributes to the low propagation loss of < 3 dB/cm for PLT film.

Using sol-gel processing method, we have prepared good optical quality thin films of lathanum modified lead titanate on Corning 7059 glass substrates. It was found that the drying conditons during the film preparation critically affects the propagation losses of the films. These films are of suitable thickness to permit optical waveguiding of visible light. In this paper, the preparation method and the optical property measurements of PLT films on Corning 7059 glass substrates were described. The drying temperature dependence of the transmittances and optical attenuations in the films will be discussed.

### II. Experimental Procedure

The procedure used for the fabrication of sol-gel PLT thin film in this study is shown schematically in Fig. 1. The precursors for the PLT solutions were lead acetate trihydrate, titanium iso-propoxide and lathanum nitrate. Lead acetate trihydrate was dissolved in methoxyethanol, and the solution was distilled to remove the water associated with the lead acetate precursor. Titanium iso-propoxide pre-dissolved in methoxyethanol were added to the lead methoxyethanol solution. The solution mixture was distilled to a final concentration of

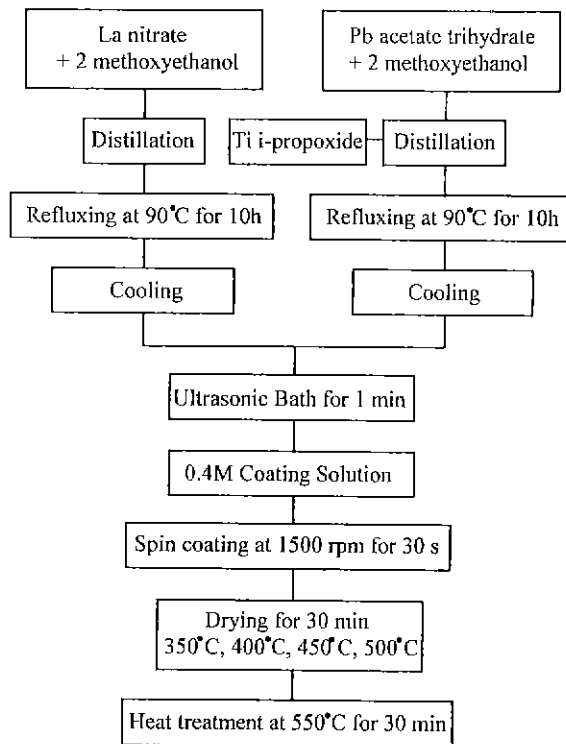


**Fig. 1.** A flow diagram for the fabrication of the solution derived PLT thin film.

about 0.4 M and then refluxed. For the preparation of a lanthanum nitrate solution, lanthanum nitrate was also dissolved in methoxyethanol, and the solution was distilled for 1 h and then refluxed. A coating solution for the film preparation was fabricated by mixing an equal volume of two solutions. Using this method, three coating solutions with different La contents were prepared. La source content (10 atomic%, 20 atomic% and 28 atomic%) in the solution was controlled because La atoms in the film took a key role in the increase of optical transmittance. The films were deposited using the spin-coating onto Corning 7059 glass substrates at 1500 rpm for 30 sec. The deposition process involved multiple cycles of the spin coating followed by intermediate drying process. With the PLT films prepared, the drying temperatures of them were controlled at 350°C, 400°C, 450°C and 500°C, respectively. The drying time was 60 minutes. The drying processes of the films were conducted on a hot plate. With the solution used, each spin coating and drying cycle contributed an average film thickness of about 0.09  $\mu\text{m}$ . The coating and the drying procedures were iterated 5 times to obtain the desired film thickness of about 0.45~0.5  $\mu\text{m}$ . After the coating and the drying procedures, all of the fabricated PLT films were heat-treated at 550°C for 30 min under air atmosphere in a furnace. A DTA/TG curve of gel powder and FT-IR spectra of the films were measured to estimate residual organics in them. The heat-treated films were charac-

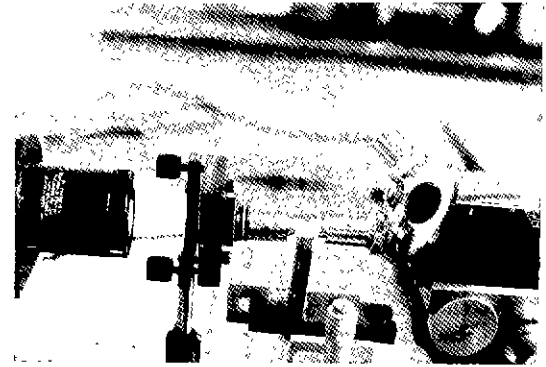
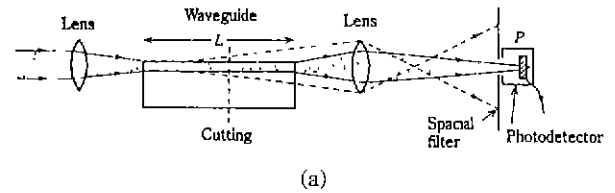


**Fig. 2.** (a) a schematic diagram and (b) the experimental set-up of the end coupling method.

terized by X-ray diffraction to determine phases present in the film. Microstructures of the films were observed with a SEM (scanning electron microscope).

The optical properties of the films, such as the transmittances and the propagation losses were estimated. The transmittance spectra of the film were measured using a Hewlett-Packard 8452 diode array spectrophotometer. The end coupling method<sup>9)</sup> was used to determine the excitation of a guided mode. Fig. 2(a) shows a schematic illustration of the end coupling method in which laser beam focused by a lens is fed onto an end of the film. The high-quality-defectless end face is prepared by cleaving the film. The propagation losses of the films were measured with the cut back method.<sup>12)</sup> Instead of the screen to observe the output image, a static laser power detector was used to measure the quantitative values of the light intensities. Fig. 2(b) shows the experimental set-up for the optical coupling between the film and the laser beam. The laser beam with Gaussian intensity distribution was fed onto the end face of film through a 40 $\times$  lens with a working distance of approximately 200  $\mu\text{m}$ . The spot size of the input beam was about 10  $\mu\text{m}$ , and therefore much of the light was lost at the input facet.

### III. Results and Discussion

To estimate the thermal decomposition characteristics of the PLT gel powder, the DTA/TG curve of the gel powder with 20 at.% La was measured under a heating rate of 5°C/min and air atmosphere. Fig. 3 illustrates

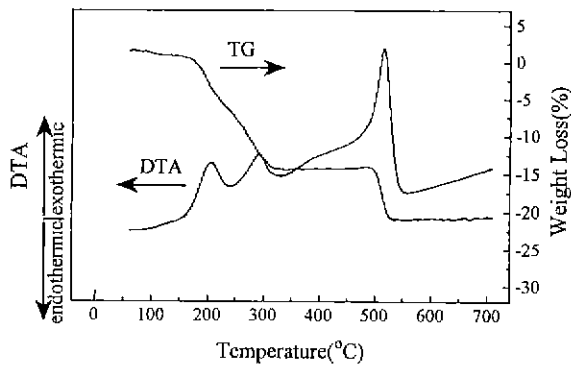


Fig. 3. DTA/TG curves of the dry gel of the PLT solution with 20 at.% La.

the DTA/TG curves of the dry gel of the PLT solution. Three exothermic peaks at 200°C, 280°C and 490°C are observed. The peaks at 200°C and 280°C are attributed to the decomposition of the metalorganic compound and the creation of CO<sub>2</sub> and H<sub>2</sub>O. The peak at around 490°C is attributed to the decomposition of the residual organics and possible crystallization of the amorphous film. However, the precise crystallization temperature cannot be determined because the crystallization peak is embedded into the decomposition peak of the residual organics. In the case of the TG curve, first weight loss of the gel powder occurs between 200°C and 280°C. Second weight loss of the gel powder occurs drastically at the temperature of around 500°C. However, the weight of the gel powder remains constant in the temperature region between 300°C and 490°C.

Fig. 4 shows the FT-IR spectra of the PLT thin films dried at different drying temperatures. Various absorption peaks representing different chemical bonds, such as CH<sub>3</sub>C, CO, COO and H-OH, are observed in the case of the gel film which was dried at 80°C on a hotplate. The film dried at 300°C shows the absorption peaks due to CO, COO and H-OH bond. As the drying temperature increases, the peak intensities of CO, COO and H-OH bonds decrease gradually. At the temperature of more than 400°C, the samples show the absorption peaks of CO<sub>2</sub> which was trapped in the films due to burning-out. The residual organics and the trapped CO<sub>2</sub> may cause the formation of the micropores which lead the decrease of the density and the refractive index. From above result, it is known that the residual organics in the film decrease gradually in the temperature region between 300°C and 500°C, which is different from the gel powder.

The phase and the crystal orientation of the films were characterized by the X-ray diffraction analysis. Fig. 5 shows the X-ray diffraction patterns of the films with various La contents. In all cases, the films mainly consist of perovskite phase, and pyrochlore phase is not observed within a resolution limit of the XRD. The XRD patterns of all the PLT films show no significant (*h*00) and (00*l*) peak split, which indicates that the phase is

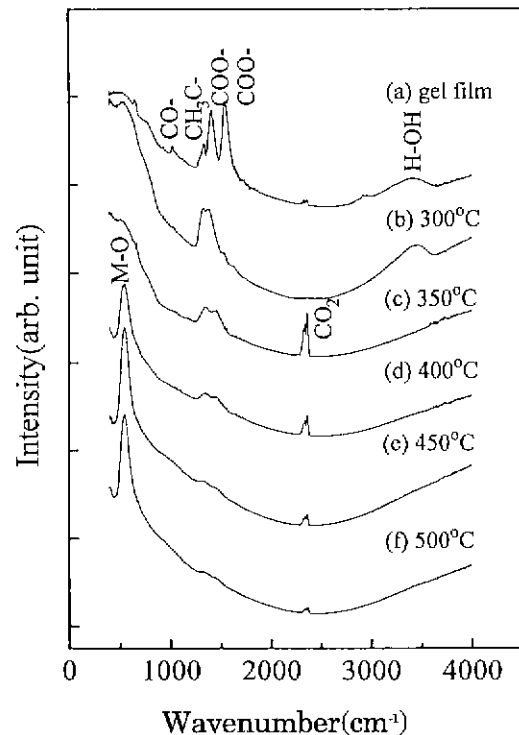


Fig. 4. FT-IR spectra of the PLT thin films dried at different temperatures for 30 min.

not tetragonal. The observed discrepancy in the peak split between the bulk and the film may be due to the thermal history difference and/or the substrate used in the film. All the films show the random crystal orientation, which is due to the substrate used in the sol-gel processing.

Fig. 6 shows the SEM images of the microstructures of the PLT films with various La contents. The surface of the films seems to be smooth and apparently void free. The film with 10 atomic% La has grain sizes of 700Å~800Å. The grain size of the film decreases as the La content in the film increases, which may indicate that the PLT film with higher La content had relatively larger number of the nucleation sites. However, some cracks are shown in the case of the film with 28 atomic% La. Because of these cracks and consequent high propagation loss, the PLT film with 28 atomic% La is not suitable for the optical waveguide applications. Fig. 4(d) shows an SEM image of the fracture surface of the film with 20 atomic% La. The film thickness is uniform throughout the specimen, which is one of the major advantages of the sol-gel processing. The uniform film thickness and the void free microstructure will confirm stable light propagation in the film without significant light scattering loss.

The transmittance spectra of the films were measured with a HP8452 diode array spectrophotometer. Fig. 7 shows the transmittance spectra of the PLT films with various La contents. All the films were heat treated at 550°C for 30 min. The oscillations in the spectra are due

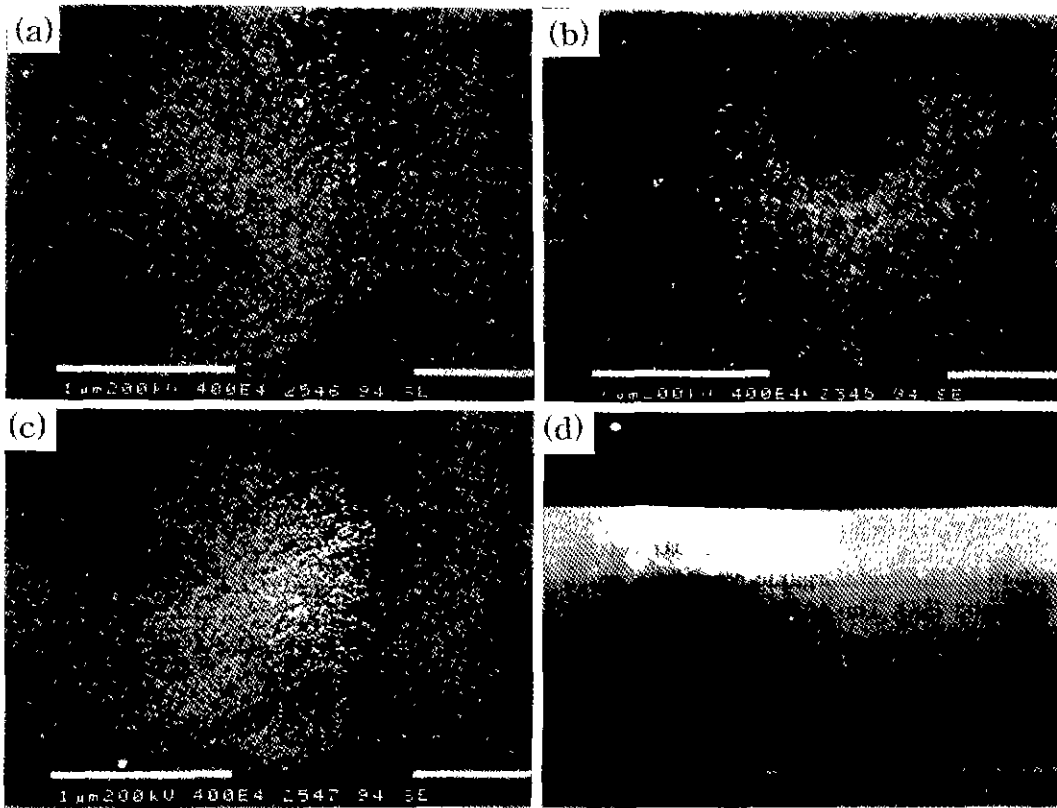


Fig. 5. X-ray diffraction patterns of the PLT films having various La contents.

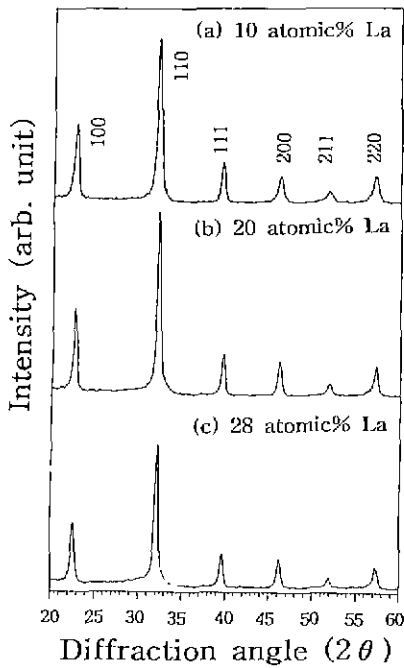


Fig. 6. SEM image of the microstructures of the surfaces of PLT films having different La contents: (a) 10 atomic %, (b) 20 atomic %, (c) 28 atomic % and (d) the fracture surface of the film with 20 atomic % La.

to the interference the reflected beams between the film surface and the film-substrate interface. The wavelength

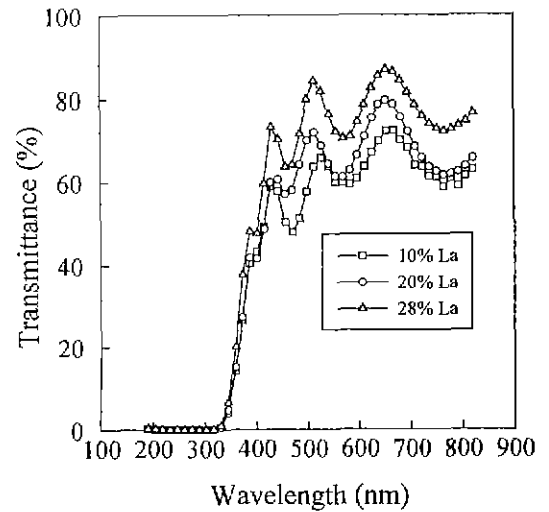


Fig. 7. Transmittance spectra of the PL films having various La contents heat-treated at 550°C for 30 min.

difference between peaks due to constructive interference depends on the film thickness and the refractive index. Fig. 7 shows the typical spectra which correspond to the films with the thickness of around 0.45 μm. In all cases, the absorption edges are observed at the wavelength of around 340 nm which corresponds to the optical band gap of 3.6 eV. The average transmittance of the film increased as the La content increased.

It has been reported that the light scattering decreases as the grain size decreased in the grain size range being much smaller than the wavelength of the light.<sup>13)</sup> As shown in Fig. 6, the grain size decreased as the La content increased. As the grain size decreased, the light scattering decreased, and the transmittance increased. Even though the PLT film with 28% La have the highest transmittance, it can not be employed for the optical waveguide application because of its cracks. Therefore, we selected the film with 20% La to apply the films for the optical waveguide.

Fig. 8 shows the transmittance spectra of the PLT films fabricated at different drying temperatures for 30 min. The average transmittance of the film increased as the drying temperature increased. The observed average transmittance trend may be associated with the residual organics and the density of the film. The solvent in the wet film is evaporated at the drying temperature. However, the residual organics in the film does not burn out completely at the drying temperature. These residual organics remain accumulated in the film throughout the repeated coating and drying process and, then, are burned out in the final heat treatment. Some of the residual organics may serve as source of voids and micropores in the final film after the film is finally heat treated. The voids and micropores serve as source of light scattering, so that the denser film may show higher transmittance. The amount of the residual organics decreased as the drying temperature increased, and the density and the transmittance of the film increased with the drying temperature.

The waveguiding characteristics of the PLT thin film were investigated with the end coupling method. Fig. 9(a) shows a scene of an end coupling between the PLT film and the laser beam. A left bright spot is the scattered beam at one end face of the PLT film, and a bright

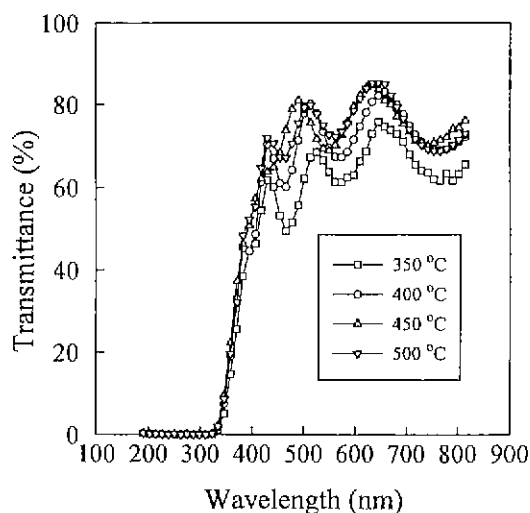


Fig. 8. Transmittance spectra of the PLT films dried at different drying temperatures for 30 min and heat-treated at 550°C for 30 min.

straight line is the light passage in the film. In the case of the film having the high optical attenuation, the brightness of the light line weakened drastically as the distance increased from the input facet. The observed output pattern of a film is shown in Fig. 9(b). Upper bright line of the image is the guided optical mode sent through the PLT film. Most samples could propagate the laser beam and create the output patterns. However, all of these samples cannot be used in the waveguide applications. The propagation loss of the film must be low ( $< 3$  dB/cm) for the waveguide applications.

The propagation loss of the film was measured using the cut-back method. In practice, however, it is rather difficult to prepare many waveguides having equal quality and different lengths. Therefore, the measurement was done by cutting a sample to change the length. We observed the guided mode images of the films on a screen before and after cutting. The output pattern of the cut sample was brighter than that of the as-received sample. The brightness of the optical mode also increased as the drying temperature increased. Instead of the screen, a static laser power detector was used to measure the quantitative values of the light intensity. The measured intensities of the output modes were  $10^{-2}$  mW order. Compared with the intensity of the He-Ne laser beam: 10 mW, the coupling efficiency between the film and the laser beam was very weak. The propagation loss of the film were obtained from the following e-

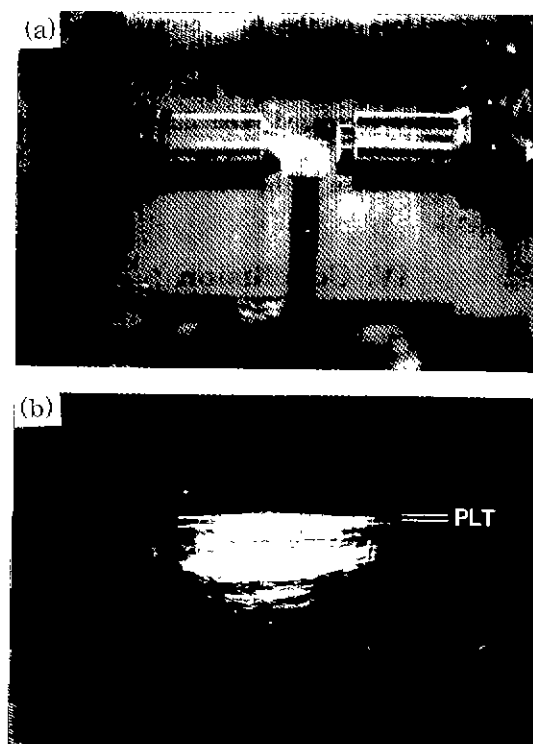
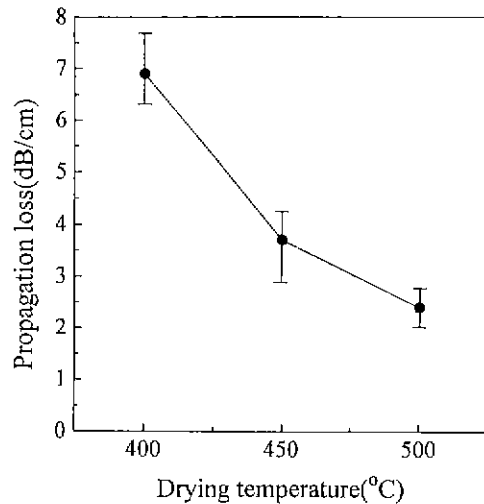


Fig. 9. (a) A scene of the end coupling between the film and the laser beam, and (b) an image of the observed output pattern.



**Fig. 10.** Propagation losses of the PLT films dried at different drying temperatures for 30 min and heat-treated at 550°C for 1 h.

equation<sup>13)</sup>:

$$\alpha = |10 \log(P_1/P_2)/(L_1 - L_2)|, \quad (1)$$

where  $L_1$  and  $L_2$  (cm) are the film lengths before and after cutting, and  $P_1$  and  $P_2$  are the beam intensities measured before and after cutting, respectively.

Fig. 10 shows the average propagation losses of the PLT films fabricated at different drying temperatures. In the case of the film dried at 350°C, we could not measure the propagation loss of the film because the optical modes were not observed due to the high optical scattering. The propagation loss of the film decreased as the drying temperature increased. The film dried at 500°C have a propagation loss of 2.4 dB/cm. These observations are consistent with those of the transmittance spectra of the films.

#### IV. Conclusion

Using the sol-gel processing method, the PLT thin films of lanthanum modified lead titanate on Corning 7059 glass substrates have been prepared. The amount of the residual organics in the film decreased as the drying temperature increased. All of the films consists of mainly

perovskite phase and shows the random crystal orientation. The grain size of the film decreased as the La content in the film increased. Some cracks were observed in the case of the film with 28 atomic% La. The transmittances of the films increased with the La content and the drying temperature. It was found that the drying temperature during the film preparation critically affected the propagation losses of the films. The propagation loss of the film decreased as the drying temperature increased.

#### Acknowledgement

The authors sincerely appreciate the financial support from KOSEF (Funding No. 94-0300-06-01-3).

#### References

1. T. Tawaguchi, H. Adachi, K. Setsune, O. Yamazaki and K. Wasa, *Appl. Opt.*, **23**[13], 2187 (1984).
2. H. Adachi, T. Kawaguchi, K. Setsune, K. Ohji and K. Wasa, *Appl. Phys. Lett.*, **42**, 867 (1983).
3. H. Adachi, T. Mitsuyu, O. Yamazaki and K. Wasa, *J. Appl. Phys.*, **60**, 736 (1986).
4. A. B. Wagner, S. R. J. Brueck, and A. Y. Wu, *Ferroelectrics*, **116**, 195 (1991).
5. V. E. Wood, J. R. Busch, S. D. Ramamurthi and S. L. Swartz, *J. Appl. Phys.*, **71**[9], 4557 (1992).
6. G. Teowee, C. D. Baertlein, E. L. Quackenbush, S. Motakef, J. M. Boulton and D. R. Uhlmann, *SPIE Proc.*, **2288**, 599 (1994).
7. G. Teowee, J. M. Bouton, S. Motakef, D. R. Uhlmann, B. J. J. Zelinski, R. Zanoni and M. Moon, *SPIE Proc.*, **1758**, 236 (1992).
8. P. F. Baude, C. Ye, T. Tamagawa and D. L. Polla, *J. Appl. Phys.*, **73**, 7960 (1993).
9. P. F. Baude, J. S. Wright, C. Ye, L. F. Francis, and D. L. Polla, *MRS Symp. Proc.*, **343**, 445 (1994).
10. G. R. Fox and S. B. Krupanidhi, *J. Appl. Phys.*, **74**[3], 1949 (1993).
11. T. Katayama, M. Shimizu and Tadashi Shiosaki, *Jpn. J. Appl. Phys.*, **32**, 3943 (1993).
12. I. P. Kaminow and L. W. Stulz, *Appl. Phys. Lett.*, **33**[1], 62 (1978).
13. D. S. Yoon, J. M. Kim, K. C. Ahn and K. No, *Integrated Ferroelectrics*, **4**, 93 (1994).